Common and Specific Determinants for Fibroblast Growth Factors in the Ectodomain of the Receptor Kinase Complex†

Fen Wang,‡ Weiqin Lu,‡ Kerstin McKeehan,‡ Khalid Mohamedali,‡ Jerome L. Gabriel,§ Mikio Kan,‡ and Wallace L. McKeehan*,‡

Center for Cancer Biology and Nutrition, Institute of Biosciences and Technology and Department of Biochemistry and Biophysics, Texas A&M University, Houston, Texas 77030, and Department of Biochemistry, Temple University School of Medicine, 3420 North Broad Street, Philadelphia, Pennsylvania 19140

Received July 21, 1998; Revised Manuscript Received November 2, 1998

ABSTRACT: The assembly and activation of oligomeric complexes of FGF, the transmembrane receptor kinase (FGFR), and heparan sulfate transmit intracellular signals regulating growth and function of cells. An understanding of the structural relationships between the three subunits and their redundancy and specificity is essential for understanding the ubiquitous FGF signaling system in health and disease. Previously, we reported that a primary heparin or heparan sulfate binding site resides in a distinct sequence in immunoglobulin (Ig)-like module II of the three modules of FGFR. Here we report that in the absence of flanking sequences, isolated Ig module II of FGFR1 supports the binding of FGF-1, FGF-2, and FGF-7 in respective order of affinity. None of the three FGFs detectably bind Ig module I or the IIIb and IIIc splice variants of Ig module III in the absence of flanking sequences. Ig module I and the C-terminus of Ig module III are dispensable for high-affinity binding of FGF-1, FGF-2, and FGF-7. Alterations in highly conserved Ig module II in the heparin binding domain and substitution of individual sequence domains spanning the entire sequence of Ig module II with those from Ig module I obliterated FGF binding. Addition of a specific number of FGFR sequences to the C-terminus of Ig module II resulted in a gain in affinity for FGF-7. Several site-specific alterations in the C-terminus of full-length FGFR1IIIc, an isoform that otherwise absolutely rejects FGF-7, resulted in gain of FGF-7 binding. These results suggest that a complex of Ig module II and heparan sulfate is the base common active core of the FGFR ectodomain and that flanking structural domains modify FGF affinity and determine specificity.

The fibroblast growth factor (FGF)[1] family is a ubiquitous family of intrinsic tissue regulators in development and adult homeostasis (*1*, *2*). Consequently, defect and dysfunction in members of the family are predicted to be involved directly or indirectly in most tissue-specific pathologies. Oligomeric complexes of FGF polypeptides, FGF receptor kinases, and heparan sulfate combine to transmit intracellular signals (*1*). The FGF polypeptides currently consist of 19 genetically distinct homologues. The FGFR kinase component is encoded by four genes, but extensive diversity in products from a single gene results from alternative splicing (*1*−*3*). The peri-cellular heparan sulfate component, which is poorly characterized, is predicted to be equally diverse (*4*). The ectodomains of different FGFR isoforms, when combined with highly sulfated heparin, the mimic of heparan sulfate from the tissue matrix, exhibit both cross-reactivity and specificity for different FGFs (*5*, *6*). An understanding of the structural determinants in the three subunits of the FGFR complex underlying both cross-reactivity and specificity is essential for design of tissue- and disease-specific agonists and antagonists. In lieu of direct structural data on members of the FGF family other than FGF-1 and FGF-2, two types of hypothetical atomic models have been employed to guide structure−function analyses of FGF and the FGFR kinase ectodomain. One type is based on the growth hormone ligand−receptor complex (*7*, *8*) with a stoichiometry of 1 FGF:2 FGFR:1 heparan sulfate and the other type a stoichiometry of 1 FGF:1 FGFR with one or two chains of heparan sulfate by bridging FGF, FGFR, or ternary complexes of FGF−FGFR (*4*, *9*−*14*).

In previous reports, we have demonstrated that the primary heparin or heparan sulfate binding domain resides in Ig module II of the FGFR ectodomain which, due to splicing, can be comprised of three or two Ig modules (*4*, *11*, *15*). Although it is not essential for FGF or heparin binding, alternately spliced Ig module I interacts with modules II and III to alter the affinity for both FGF and heparin (*16*). In addition, removal of over 80% of the C-terminus of Ig module III by proteolysis or mutation had little effect on

† This work was supported by U.S. Public Health Service Grants DK47039 and DK35310 from the National Institute of Diabetes and Digestive and Kidney Diseases, and Grant CA59971 from the National Cancer Institute.

* To whom correspondence should be addressed at Albert B. Alkek Institute of Biosciences and Technology, Texas A&M University, 2121 W. Holcombe Blvd., Houston, TX 77030-3303. Telephone: 713-677-7522. Fax: 713-677-7512. E mail: wlmckeehan@ibt03.tamu.edu.

‡ Texas A&M University.

§ Temple University School of Medicine.

[1] Abbreviations: FGF, fibroblast growth factor; FGFR, FGF receptor kinase; FGFR1−4, type 1 through 4 of the FGFR kinases; FGFRα, splice variant of FGFR containing three Ig modules; FGFR*β*, splice variant of FGFR containing two Ig modules; PCR, polymerase chain reaction; G-box, FGF glycine box; GSH, glutathione; GST, glutathione-*S*-transferase; Sf9, *Spodoptera frugiperda*; SDS−PAGE, sodium dodecyl sulfate−polyacrylamide gel electrophoresis; PBS, phosphate-buffered saline.

10.1021/bi981758m CCC: $18.00
Published on Web 12/12/1998

the remainder of the FGFR ectodomain to bind FGF-1, FGF-2, and FGF-7 and concurrently removed restriction on FGF-7 binding by the IIIc splice variant of FGFR (*4, 5*). More recent results suggest that only Ig module II in the absence of sequences N-terminal or C-terminal to it retains the ability to bind heparin and one or more FGFs (*15*).

In the current study, we report results of a series of site-directed mutagenesis experiments aimed at defining the relative role of each Ig module and flanking sequences in the common and specific binding of FGF-1, FGF-2, and FGF-7. In the absence of flanking sequences, Ig module II supported the binding of FGF-1 with nearly equal affinity to FGFR1β which contained both modules II and III. Although the affinity was reduced, FGF-2 and FGF-7 also bound to the isolated Ig module. None of the three FGFs bound Ig module III from the FGFR1IIIc or FGFR2IIIb isoforms in absence of flanking sequences. Most sequence domains in Ig module II could not be substituted with corresponding sequences from structurally homologous, but inactive, Ig module I.

Guided by a model of a ternary complex of FGF, the FGFR1β ectodomain, and a hexadecameric heparin chain (*11, 12*), site-directed mutagenesis and functional analysis suggested three sites that contribute to the absolute rejection of FGF-7 by FGFR1IIIc and, therefore, give rise to the specificity of FGF-7 for the FGFRIIIb splice variant. Although a global disruption of the dimerization domain which connects modules II and III interferes with FGF binding, mutation of several single residues, including two (S162W and P163R) that cause skeletal abnormalities, does not affect FGF binding. These results confirm that a complex of Ig module II and heparan sulfate is the base common core of the FGFR ectodomain and that both constitutive and alternately spliced flanking domains modify FGF affinity and specificity by both positive and negative forces.

MATERIALS AND METHODS

Oligonucleotide Primers. Oligonucleotides that have not been described elsewhere are listed below, and were purchased from Integrated DNA Technologies, Inc. (Coralville, IA). Numbering is based on +1 for the first nucleotide of the initiation codon in the FGFR1β cDNA. Restriction sites are underlined, and nucleotides not in the coding sequence for FGFR are in lower case.

Construction of Recombinant FGFR cDNAs. cDNAs coding for the full-length FGFR1α1, FGFR1β1, and FGFR2β1 tyrosine kinases and other mutants have been described (*4, 5, 15*−*17*). The mutant cDNA fragments were generated by the polymerase chain reaction (PCR) using the above primers and FGFR cDNA templates as described (*5, 15*−*18*).

The PCR fragment for R1S1 was generated with primers pS1 and p2d (*17*), and R1β as the template. After treatment with *Bgl*II and *Taq*I, the mutant fragment was ligated with the upstream cDNA fragment digested from R1$\alpha\Delta$IIAH at the *Bgl*II site and the downstream R1 cDNA fragment at the *Taq*I site, resulting in a cDNA coding for the translation initiation site through 26 amino acid residues downstream of the transmembrane domain as described (*4, 5, 16*). Primers p1a and PS3 were used to generate the mutant fragment for R1S3 with R1$\alpha\Delta$IIAH template. The cDNA was treated with

p1a: CGAGCTCACTGTGGAGaATtCATG

p2d: CCCATTCACCTCGATGTGCTT

p6T: atatgaattcGTGCACAGCCATCTGGCGTGGAA

pB2: gcctgaattcAGCTTGTGCACAGCCGGCTGGCT

pB3: TGGATCAAACATGTCGAAAAGAAC

pD9: GGGGAGAGtcgacGAAACATTGACGGA

pD10: TGGAGCTGtcgacATACGGTTTGGTTT

pD11: CCTGCAaagcttTCCACGGTGGTCGGA

pD12: GAAGTCTGGCTTCTTGGTaccGGTCTT

pS1: agcaGCCCCTCGGGCAGCATCAACCACACA

pS3: TTTTTCCAATTCTGTGGCTTTCCGCCAGCTGCAC

pS4: AGCCACCGCACTGGCATCACA

pS5a: GGAGTCTGCGGGCACCACAGAGTCCATTAT

pS5b: ATAATGGACTCTGTGGTGCCCGCAGACTCC

pS6: ACTGCCCGAGGGGCTCTCCACAATGCA

p70a: TCCCCtttaAAGATGGAAAAGAAA

p70b: TTTCTTggCCATCTTTTCTGGGGA

p135a: TCTGcCAAGGGCAACTACACaTGCATT

p135b: AATGCAGGTGgcGTTGCCCTTGTCAGA

p157a: CAGCTGctgGTCGTGGAGCGGTCC

P157b: GGAtCGaagCACGACCTCCAGCTG

p162a: GTGGAGCGGTCCCgtCACCGGCCC

p162b: CGGTGAGGccACCGCTCCACGAC

p164a: CGGTCCCCTtTCCGGCCCAT

p164b: ATGGGCCGGAaAGGGGACCG

p185a: AGCAACGTGGcGTTCATGTGT

p185b: ACACATGAACgCCACGTTCGT

p193a: AAGGTGTACAGTGcACCGCAGCCGCAC

p193b: GTGCGGCTGCGGTgCACTGTACACCTT

p197a: CAGCCGTTCATCCAGTGGCTAaAGCACATCGAG

p197b: CTCGATGAACTtTAGCCACTGGATGTGCGGCTG

p223a: AAGGTCCTGgcGCACTCGGGGATA

p223b: TATCCCCGAGTGCgcCAGGACCTT

p223c: TACCTCAAGGTCCTGgcGGCCGCC

p224a: AATACCACCGACAAAGAGATGGAG

p224b: CTCCATGTCGGTGGTATTAACTCCactatgCTT

p232a: GTTAACACCACCGACATGGAGGTG

p232b: CACCTCCATGTCGGTGGTGTTAAC

*Pst*I and *Bst*XI, ligated with the downstream sequence at the *Bst*XI site, and cloned into pBluescript SK at *Eco*RI and *Pst*I sites. The mutant fragment for R1S4 was generated with primers pS4 and p2d (*4*) and R1$\alpha\Delta$IIAH template. After treatment with *Bst*XI and *Taq*I, the PCR fragment was ligated with the flanking sequence of R1β and cloned into pBluescript SK vector at *Pst*1 and *Eco*R1 sites. For R1S5, two PCR fragments were generated with primers p1a and pS5a and R1β template, and primers pS5b and p2d and R1S4 template, respectively. The PCR fragments served to generate a mutant fragment with primers p1a and p2d, which was

treated with *Pst*I and *Taq*I, ligated with the downstream sequence, and cloned into pBluescript SK vector at *Pst*I and *Eco*RI sites. The mutant fragment for R1S6 was generated with primers p1a and pS6 and R1β template. The PCR fragment was treated with *Bgl*II and *Pst*I, ligated with the downstream sequence from R1S4, and cloned into pBluescript SK vector at *Pst*I and *Eco*RI sites. R1S2 was generated by ligation of the 5′ sequence of R1S3 and the 3′ sequence of R1S6 at the *Bst*XI site. R1S7 and R1S8 were generated by ligation of the 5′ sequence of R1S5 or R1S6 with the 3′ sequence of R1S1, respectively.

The PCR fragments for R1T224H,A225S and R1T224H, A225KE were generated with p157a and p224b, p224a and p6 (*4*) and R1β template, respectively. The PCR fragments served as the templates to generate the mutant fragment with p157a and p6. The mutant fragment for R1ΔKE was generated with the same strategy except with mutant primer p232a and p232b. The PCR fragments were treated with *Eco*R1 and *Taq*I, ligated to the 5′ sequence from R1b at the *Taq*I site, and cloned into pBluescript SK at *Pst*I and *Eco*R1 sites. The cDNAs coding for R1T224H,A225S and R1T224H, A225S,ΔKE were distinguished by treatment with *Bst*X1.

The PCR fragment for R2βIIIcK223A was generated with p223c and pB2 (*5*) and R2βIIIc template. Two PCR fragments for R2bIIIbK223A were generated with p223a and pB2, and p223b and pB3 with R2IIIb template, which served as the templates for generation of mutant fragment with pB2 and pB3. The PCR fragments were treated with *Eco*O109I and *Apa*lI, ligated with the flanking sequence at *Eco*O109I and *Apa*lI sites, and cloned into pBluescript SK vector at the *Pst*I site.

Two PCR fragments for R1E70A and R1E73A were generated with p1a and p70b, p70a and p157b and R1β template, which are being used as the templates for generation of the mutant fragment with p1a and p157b. After treatment with *Pst*I and *Bst*XI, the mutant fragment was ligated with the downstream sequence and cloned into pBluescript SK vector at *Pst*I and *Eco*RI sites. The following asymmetric paired primers were used for the indicated mutants, using the same 5′-flanking primer (p70a) and 3′-primer (p224b) with R1β template as described (*5*, *18*). P135a and p135b were used for R1D135A and R1Y139A; p157a and p157b for R1D157A and R1E160A; p162a and 162b for S162W and P163R; p164a and p164b for R1H164F; p185a and p185b for R1E185A; p193a and p193b for R1D193A; p197a and p197b for R1H197F and R1H203F. The PCR fragments were treated with *Taq*I and *Bst*XI, ligated to the flanking sequence, and cloned into pBluescript SK vector at *Pst*I and *Eco*RI sites.

Primers pD9 and p1a (*5*) with R1α template were used for generation of R1$\alpha\Delta$II$-$III, pD10, and p1a with R1β template and were used for R1$\beta\Delta$II$-$III. The PCR fragments were treated with *Pst*I and *Hin*cII, ligated with the downstream sequence coding for the transmembrane domain and glutathione-*S*-transferase (GST) as described (*15*). Primers pD11 and pD12 were used for generating R2βIIIbΔIIGST. The PCR fragment was treated with *Hin*dIII and *Kpn*I, ligated with the cDNA coding for the R1 signal peptide at the 5′-end and GST at the 3′-end as described (*15*), and cloned into pBluescript SK vector.

The complete sequence of mutant cDNA fragments generated by the PCR and the sequence across ligation sites with flanking wild-type FGFR cDNA sequence were determined. After verifying the sequence, all the cDNA constructions were excised and cloned into baculoviral transfer vector pVL1393 or pVL1392, or mammalian expression vector pcDNAzeo 3.1 (Invitrogen, San Diego, CA) or p91023 (*4*, *5*).

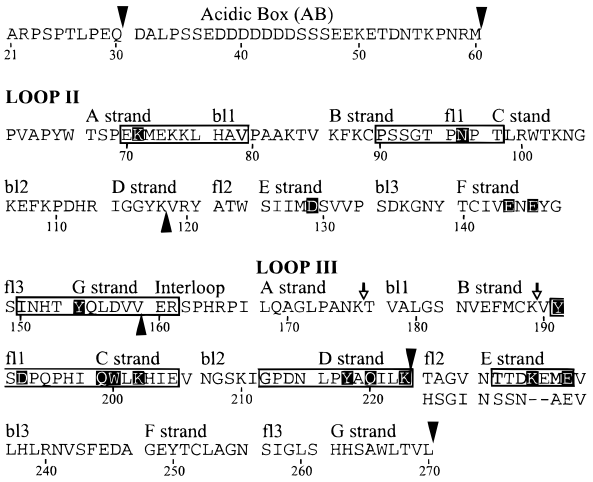

FIGURE 1: Assignment of structural units to the FGFR ectodomain by homology modeling. Atomic models of a complex of variants of the FGFR ectodomain through Ig module III, a hexadecameric chain of fully sulfated heparin, and FGF-1, FGF-2, and FGF-7 were constructed as described under Materials and Methods. Sequence domains of Ig modules II and III and the interloop sequence of FGFR1β were assigned using a template constructed from the X-ray coordinates for a constant Ig unit from the light chain of IgG1 (*5*, *9*, *21*). From this assignment, Ig modules II and III are comprised of residues 61$-$159 and 168$-$270, respectively. The sequence of human FGFR1βIIIc grouped into the indicated structural domains using Ig module nomenclature (capital letters = β-strands; bl = back inter-strand loops; fl = front inter-strand loops) is shown. Sequence domains that are interactive with FGF in the models are boxed, and residues with side chains within 3 Å of FGF residues are in inverse print. Exon junctions are noted by solid triangles. Arrows indicate tryptic modification sites and the C-terminus of constructs that do not and do bind FGF-1, FGF-2, and FGF-7, respectively, described in the text and ref *5*. The fl2-E sequence from FGFR2IIIb is shown below that of FGFR1IIIc. Numbering throughout the manuscript is based on the FGFRβ isoform beginning with the initiator methionine unless otherwise noted.

Expression of Recombinant FGFR Variants. Recombinant baculoviruses were prepared for expression in *Spodoptera frugiperda* (Sf9) insect cells as described (*4*, *5*, *15*, *19*). The titer of recombinant virus was determined, and each recombinant viral stock was standardized by analysis of the level of expression of antigen determined by immunoblot. Transient transfection of COS-7 cells and stable transfection of DT3 cells were performed as described (*5*, *20*). The expression levels of transfected cells were determined by surface antigen assay with anti-FGFR1 antiserum A50 (*5*, *9*). Ligand binding and Scatchard analyses for COS-7 cells were performed as described earlier (*4*, *5*, *17*).

Binding of FGF to Recombinant FGFR. FGF-1, FGF-2, and FGF-7 were iodinated to a specific activity of (2$-$5) $\times$ 10^5 cpm/ng, and analysis and covalent affinity cross-linking of ^{125}I-FGF were performed as described (*4*$-$*5*, *9*, *11*, *15*$-$*22*). Binding mixtures contained 2 ng/mL labeled ligand and 2 μg/mL heparin. Binding was performed at room temperature for 2 h. For covalent cross-linking assays, the specific binding of labeled ligand was cross linked to FGFR by

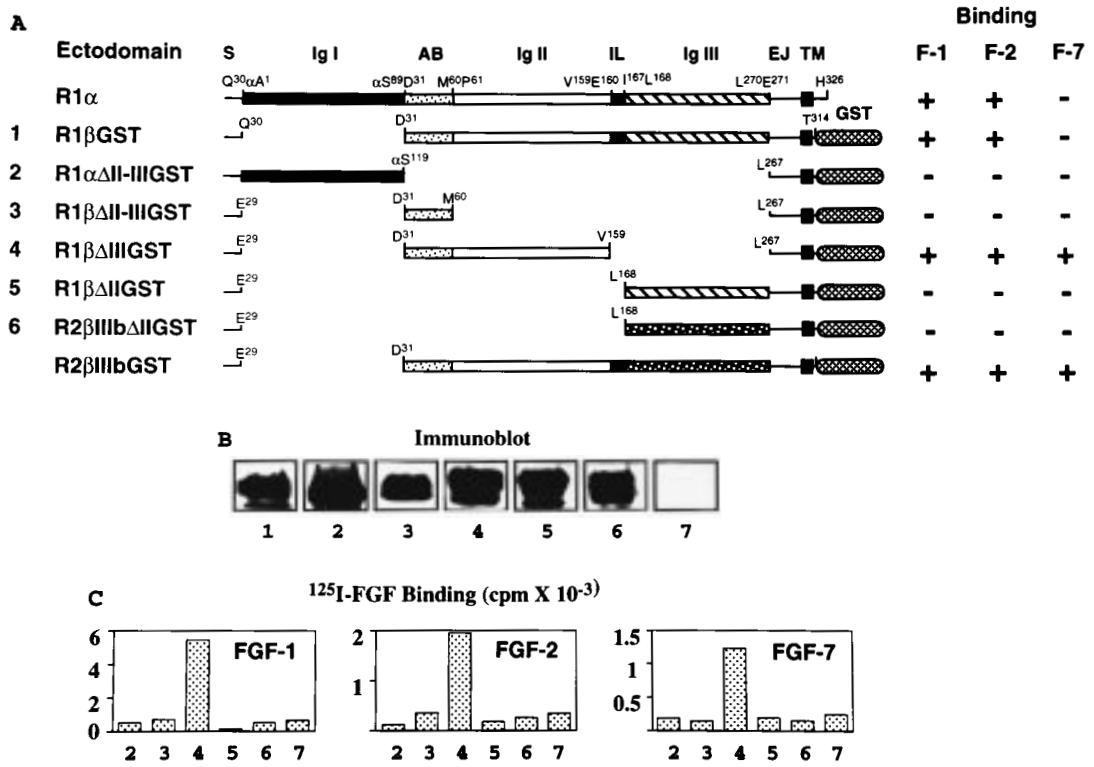

FIGURE 2: Binding activity of structural modules of the FGFR ectodomain. (A) Schematic of modular constructions. S, signal sequence; AB, acidic box; IL, the inter-Ig loop domain between Ig modules II and III; EJ, extracellular juxtamembrane; TM, transmembrane domain; GST, glutathione-*S*-transferase. A positive sign (+) indicates detectable versus undetectable (−) binding of the purified recombinant FGFR and heparin duplex. (B) Expression and immunoblot analysis. A sample of products 1−6 from (A) from 10^6 baculoviral-infected Sf9 insect cells (about 200 ng of antigen) after capture with and release from GSH−Sepharose beads was subjected to SDS−PAGE and analyzed with anti-GST antibody (A19). Lane 7 was from uninfected Sf9 cells. The major band in lanes 1−6 was at 68, 45, 31, 46, 48, and 55 kDa, respectively. (C) FGF binding to modular constructions. Specific binding of the indicated radiolabeled FGF to samples of constructions 1−6 from (A) which were anchored on GSH−Sepharose was analyzed as described under Materials and Methods. Lane 7 was from uninfected Sf9 cells. The indicated results are the mean of duplicates, and the experiment was representative of three independent trials. Binding to the control two-Ig module, FGFR1βGST [construct 1 in (A)], which is not shown, was 6000−8000 cpm for FGF-1 and FGF-2 compared to the 200−300 cpm for FGF-7 which was the background binding to uninfected cells (lane 7).

incubating with 3 mM disuccinimidyl suberate (DSS) at room temperature for 10 min.

Construction of Atomic Models. Methods for construction of a ternary complex of FGF-1, FGF-2, or FGF-7, a hexadecameric chain of heparin, and the ectodomain comprised of the two Ig modules of FGFR1βIIIc or a chimera of FGFR1β/FGFR2βIIIb have been described in detail (*11*, *12*, *21*). The complex of FGF-7 with mutated FGFR1βIIIc was built as follows: Using the FGF-1−heparin−FGFR1IIIc complex (*12*) as a template, specific mutations were introduced, and FGF-7 was then overlaid on the FGF-1 part of the complex. The new ternary complex of FGF-7−heparin−mutant FGFR1IIIc was then subjected to multiple rounds of molecular dynamics calculations, followed by energy minimization until convergence.

RESULTS

Predictions from a Molecular Model of the Ternary Complex of FGF, Heparin, and the FGFR Ectodomain. Molecular models of a ternary complex of FGF-1, FGF-2, or FGF-7, a hexadecameric chain of heparin, and the ectodomain of FGFR1βIIIc, FGFR2βIIIb, or a chimera of FGFR1β and FGFR2βIIIb were constructed as described in previous reports (*4*, *9*, *11*, *12*, *21*). All variants of the model indicate that FGF-1, FGF-2, and FGF-7 interact commonly with two of three sequence domains (A-bl1;B-fl1;fl3-G) in a complex of heparin and Ig module II (Figure 1). FGF-7 notably does not interact with the B-fl1 domain of module II. The common A-bl1 and fl3-G domains are near the N- and C-termini of module II, respectively, and therefore predict that an intact module might be required for binding of all FGFs. All three FGFs commonly interact in variants of the model ternary complex with two sequence domains (fl1-C and bl2-D) within module III, while FGF-2 and FGF-7, but not FGF-1, interact with a third domain (E) in the alternate exons IIIb or IIIc (Figure 1). As reported previously, this model predicts no important interactions with FGF in the C-terminus of module III past the E domain (*5*). A model of FGF-7 docked into a complex of heparin and FGFR1IIIc that is impossible to demonstrate experimentally suggested specific points of both spatial and charge conflicts that were not apparent in the models containing FGF-1 and FGF-2. The major spatial conflict of FGF-7 was with the fl1-C domain of FGFR1IIIc. Side chain charge conflicts between individual residues unique to FGF-7 with both the fl1-C and E sequence domains were observed. These observations were used to guide and interpret site-directed mutagenesis and experimental tests.

Isolated Ig Module II of FGFR1 Retains the Ability To Specifically Bind Heparin and FGF-1, FGF-2, and FGF-7. In previous reports, we showed that, despite the rejection of FGF-7 by a complex of heparin and the intact 2 Ig modules

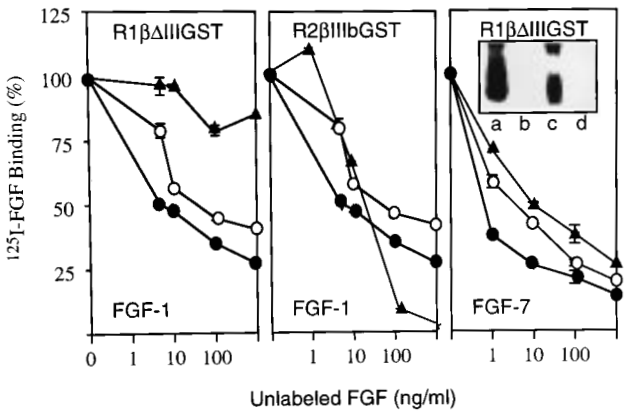

FIGURE 3: Specificity of FGF binding to isolated Ig module II. The indicated FGFR constructions were expressed in 2×10^6 Sf9 cells and immobilized on GSH−Sepharose beads, and about 200 μL of beads was suspended in 600 μL of PBS and divided into 30 portions which were used in binding assays. Assays contained a total volume of 250 μL and 2 ng/mL radiolabeled FGF indicated in the panels. Unlabeled FGF-1 (solid circles), FGF-2 (open circles), or FGF-7 (triangles) was added at the indicated concentrations. The data are the mean of duplicates and are expressed as the percentages of the binding activities without unlabeled ligands. 100% values represent 20 and 2 fmol of bound FGF-1 and FGF-7, respectively. Competitive binding to FGFR2IIIbGST (center panel) was used as a control. Inset: Covalent affinity cross-linking analysis: a, ^{125}I-FGF-1; b, ^{125}I-FGF-1 plus unlabeled FGF-1; c, ^{125}I-FGF-7; d, ^{125}I-FGF-7 plus unlabeled FGF-1. Unlabeled FGF-1 was 10 times the concentration of labeled FGF. After treatment with DSS as described under Materials and Methods, beads were collected and extracted and subjected to SDS−PAGE and autoradiography for 1 day for FGF-1 and 7 days for FGF-7. The mean of the indicated autoradiographic bands is at 63 kDa (46 kDa recombinant product and 17 kDa FGF).

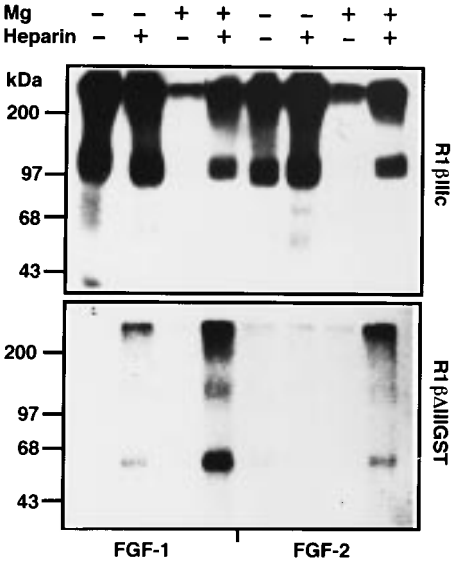

FIGURE 4: Strict heparin dependence of FGF binding to Ig module II. FGFR1βIIIc and FGFR1ΔIII-GST from 10^6 baculoviral-infected Sf9 cells were immobilized on protein A beads via A50 anti-FGFR1 antiserum (*4*) and GSH-beads, respectively. Beads were washed with 1 M NaCl in PBS, and then PBS twice, and then the beads were divided into 8 fractions after suspension in 800 μL of PBS. Immobilized constructions were introduced into the binding assays described in Figure 3 with 2 ng/mL either FGF-1 or FGF-2 in the absence or presence of 25 mM $MgCl_2$ and 2 μg/mL heparin as indicated. Covalent affinity cross-linking was analyzed as described in Figure 3. Mean of the autoradiographic bands in the upper panel is at 107 kDa (90 kDa construct product plus 17 kDa FGF). In the lower panel, the autoradiographic band at 63 kDa is comprised of the 46 kDa product plus 17 kDa FGF. The band at about 125 kDa is believed to be a dimer cross-linked through the GST dimer since no dimers in the presence or absence of FGF occur with isolated Ig module II constructs without the GST tag (15).

of FGFR1βIIIc (throughout this report reference to FGFR1 refers to FGFR1IIIc), an active core comprised of module II, the sequence connecting modules II and III, and 22 residues of Ig module III defined by homology to Ig motifs in other proteins bound FGF-7 with a similar affinity as FGF-1 and FGF-2 (*5*). However, reduction to a fragment extending only nine residues into module III past the intermodule sequence resulted in loss of binding to all three FGFs (*5*). To delineate the contribution of distinct structural modules to FGF binding in the absence of flanking sequences, we constructed and expressed a series of recombinant products comprised of distinct structural modules of the ectodomain fused to the extracellular juxtamembrane and transmembrane sequence with an intracellular GST tag (Figure 2). The binding of FGF-1, FGF-2, and FGF-7 to complexes of heparin and the constructs, either on the cell surface or isolated and immobilized to GSH-beads, was compared. Of the constructs tested, FGFR1$\beta\Delta$IIIGST comprised of only Ig module II from FGFR1 exhibited the ability to detectably bind radiolabeled FGF-1, FGF-2, and FGF-7. The relative efficiency, presumably the affinity, of binding to the isolated module II was in the order FGF-1 > FGF-2 > FGF-7. The binding of radiolabeled FGF-1 was subject to competition with unlabeled FGF-1, FGF-2, and FGF-7 in respective order (Figure 3). Although unlabeled FGF-7 competed poorly with radiolabeled FGF-1 because of its reduced affinity, all three unlabeled FGFs competed effectively with radiolabeled FGF-2 and FGF-7. Radiolabeled FGF-1, FGF-2, and FGF-7 bound the isolated Ig module II in a conformation sufficient to covalently cross-link with a 10 Å bifunctional agent (*15*, Figure 3, inset). No binding of radiolabeled FGF-1, FGF-2, or FGF-7 could be detected to Ig module I, the characteristic acidic box between Ig modules I and II, or isolated module III from FGFR1IIIc or FGFR2IIIb in binding assays (Figure 2C), or competition and covalent cross-linking analyses (results not shown). Additional experiments confirmed that the presence or absence of the acidic box domain combined with the isolated modules indicated had no effect on the outcome as reported elsewhere for the intact FGFR ectodomain (*22*).

The Stringent Heparin Dependence of FGF Binding to Ig Module II. Previously we showed that the binding of FGF to FGFR1β is conditionally dependent on heparin or heparan sulfate (*11*). Divalent cations at physiological levels present in the extracellular environment increase the dependence of the binding of FGF on heparin and, in addition, are required for the specific, high-affinity interaction of heparin with FGFR. FGFR1$\beta\Delta$IIIGST (isolated Ig module II) and intact FGFR1βGST (Ig modules II and III) were immobilized to GSH-beads and protein A beads, respectively. The binding of radiolabeled FGF-1 or FGF-2 was examined in the absence or presence of $MgCl_2$ (Figure 4). In contrast to the intact FGFR1β structure containing both Ig modules II and IIIc (Figure 4, top), the binding of FGF to isolated module II appeared unconditionally dependent on the presence of heparin (Figure 4, bottom).

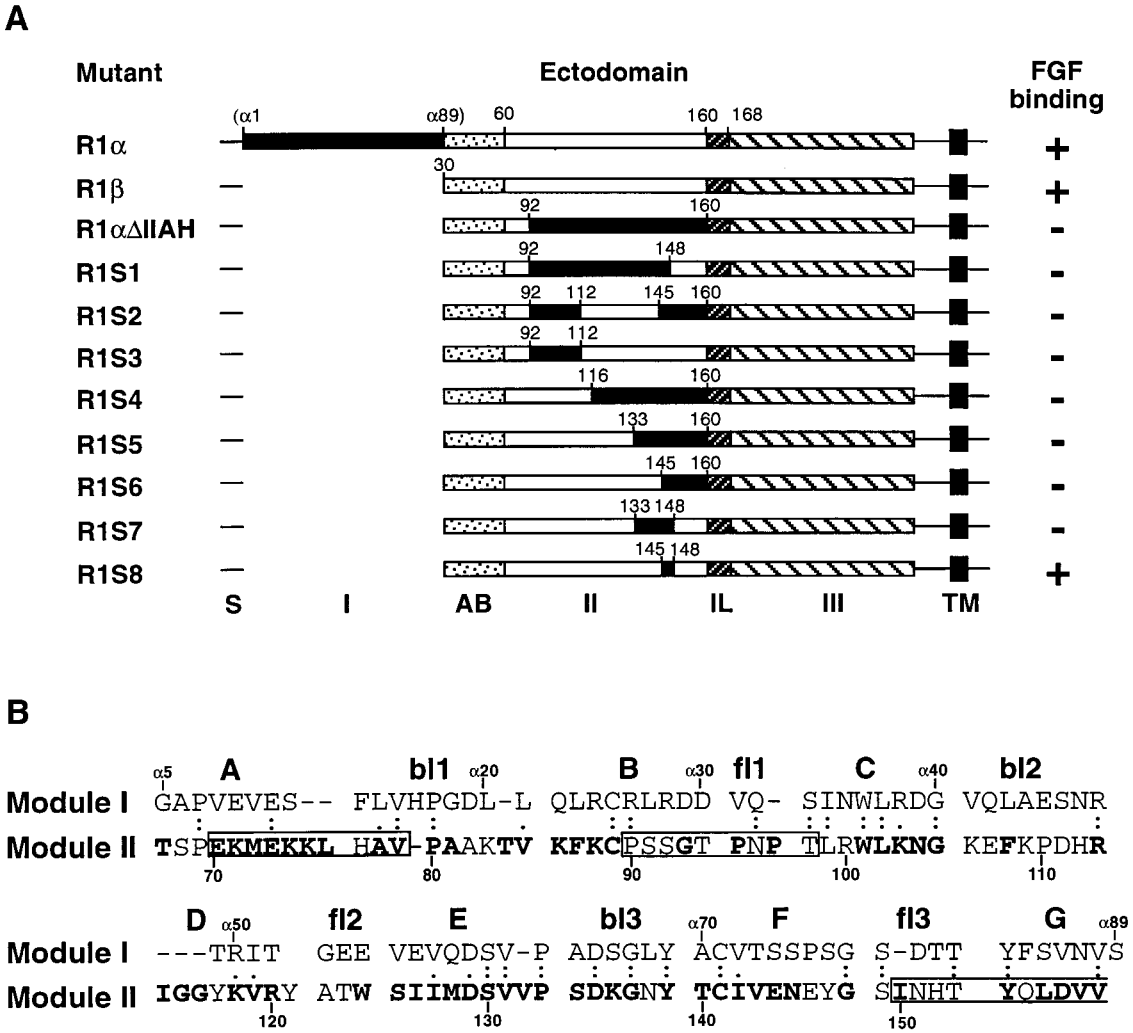

FIGURE 5: Schematic of constructions of Ig module II with substitutions from inactive Ig module I. (A) Structural modules are coded as in Figure 2. Substitutions from module I are shown in black within module II, which is otherwise white. Numbering at insert boundaries indicates amino acid residues in module II by FGFR1β numbering. (B) Sequence alignment of modules I and II. Ig homology domains are grouped as indicated. Boxed residues are FGF interaction domains indicated by molecular modeling (Figure 1). Conserved residues in module II throughout the four FGFRs are in boldface type.

Stringent Requirement for Ig Module II-Specific Sequence Domains. Sequences within Ig module II are the most conserved among structural modules in the FGFR ectodomain. Homology among the four FGFRs in human, mouse, rat, chicken, and xenopus is 65% for module II, while that for modules I and III is 17% and 51%, respectively (*1*, *2*, *9*). We have shown previously, using site-directed mutagenesis, that one of the most highly conserved sequences among FGFR near the N-terminus of module II is required for both heparin and FGF binding (*4*). To determine whether other clusters were equally essential, we constructed a series of mutants of FGFR1βIIIc in which the highly conserved domains of Ig module II were substituted with the counterpart sequences from Ig module I of FGFR1 (Figure 5). Mutant constructions were cloned, transiently expressed in mammalian COS-7 cells, and examined for binding of FGF-1 and FGF-2. Of nine mutant constructions tested, all but one (FGFR1S8) failed to bind FGF-1, FGF-2 (Figure 6), or FGF-7 (data not shown) at all.

Two additional mutants were constructed to further test the requirement for an intact Ig module II. The consensus sequence DXGXYXC surrounding the C-terminal half-cystine has been proposed to be generally important for the structure of the Ig motif; especially the tyrosine residue is involved in the major hydrophobic core, playing important roles in folding, stability, and activity of proteins (*23*), and is conserved in all three of the Ig modules in all four FGFR. The two conserved residues in the consensus domain, D135 and Y139, were substituted with alanine to generate mutants R1βD135A and R1βY139A. Substitution of Y139A abolished the binding of both FGF-1 and FGF-2, while substitution of D135A reduced the binding of both significantly, more severely in the case of FGF-1 than FGF-2 (Figure 7). The stringent requirement for an intact module II and its unique sequence domains supports the idea that the module, in contrast to modules I and III, is the primary and indispensable binding site for FGF-1, FGF-2, and FGF-7 within the two-module structure of FGFRβ.

Cooperation between the Conserved fl1-C and Variant fl2-E Domains in Ig Module III in Determination of FGF Specificity. Although sequence domains downstream of the B strand in Ig module III are not essential for the binding of heparin and FGF-1, FGF-2, and FGF-7 to FGFR, addition of only a few residues of the highly conserved and constitutive fl1-C domain caused rejection of FGF-7 with little effect on FGF-1 and FGF-2 (*5*). Molecular models of the experi-

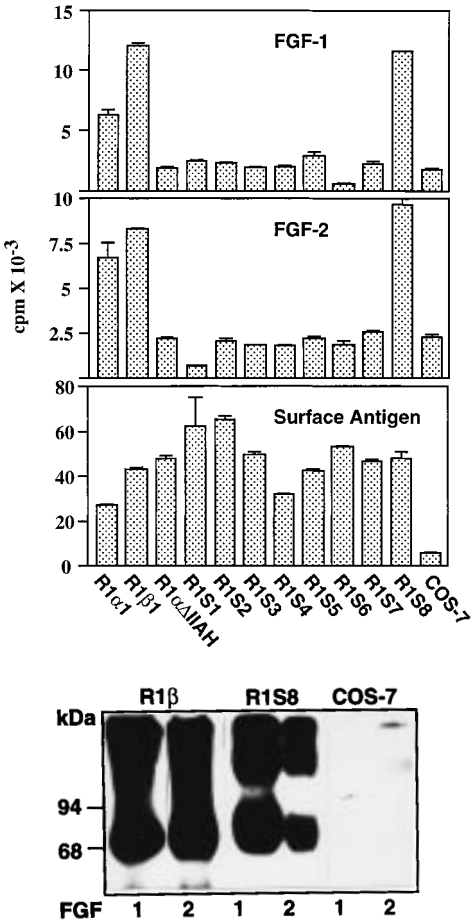

FIGURE 6: Activity of constructions with substitutions from inactive module I inserted into Ig module II. (Top panels) Membrane-anchored constructions described in Figure 5 were transiently expressed on the surface of mammalian COS-7 cells as described (*5*). After transfection, the cells were divided into three fractions for use in binding assays with radiolabeled FGF-1, FGF-2, and display of surface antigen, respectively. Surface antigen was determined with rabbit anti-FGFR1 serum A50 as described (*5*). The data are the means of duplicates with variations indicated. (Bottom panel) Covalent affinity cross-linking analysis. COS-7 cells (10^6) transfected with the indicated constructs or control vector (COS-7) described above were divided into two fractions for FGF-1 and FGF-2 covalent cross-linking analysis. Only the two active constructions are shown. The mean of the construct product is about 70 kDa (52 kDa product plus FGF).

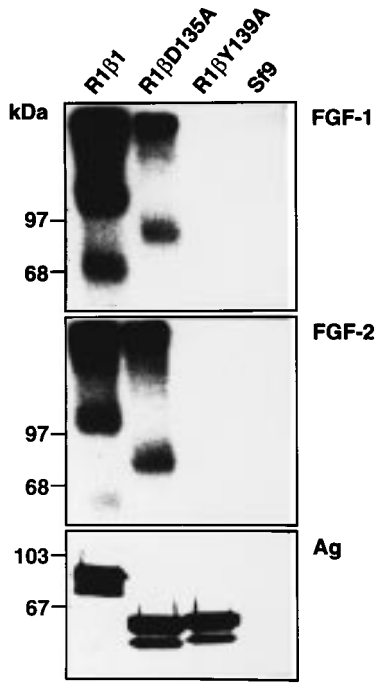

FIGURE 7: Impact of mutation of Ig motif consensus residues in module II. The indicated mutants were expressed in Sf9 insect cells, 10^4 infected cells were employed in binding assays containing radiolabeled FGF-1 or FGF-2, and 10^6 cells were lysed and used in immunoblots (Ag) using anti-FGFR1 monoclonal antibody M17A3 (*9*). Full-length FGFR1β1 radiolabeled with FGF has a mean mass of about 110 kDa. The lower band is due to proteolysis as described (*15*). The apparent mass of the three membrane-anchored antigens with truncated intracellular domain is 90, 60, and 60 kDa, respectively (bottom).

mentally impossible heparin−FGFR1βIIIc−FGF-7 complex indicate a severe spatial conflict between at least two discontinuous sequence domains of FGF-7 and the fl1-C domain (Figure 1). A screen of several alterations in the fl1-C domain in FGFR1 failed to increase FGF-7 binding. Instead, the same mutations either obliterated FGF binding altogether, selectively reduced FGF-2 binding, or, in the case of the IIIb isoforms, reduced FGF-7 binding without effect on FGF-1 or FGF-2 (*5*, Table 1). This supports the idea that this constitutive and relatively conserved structural domain is either permissive for or has a negative impact on the interaction of FGF with the module II−heparin complex.

Alternately spliced exons IIIb of FGFR2 and IIIc of FGFR1 differ in the fl2 sequence (HSGI versus TAGV) and in the E domain by the absence or presence of the dipeptide sequence KE, respectively (*3*, Figure 1). Previously, we showed that substitution of the HS with TA or insertion of the KE sequence in the FGFR2IIIb exon completely abolished the binding of FGF-7 without effect on FGF-1 binding (*5*). To test whether the counterpart alterations in the FGFR 1IIIc exon would confer ability to bind FGF-7, we constructed an FGFR1βIIIc in which the TA sequence in the fl2 domain was replaced with HS or the KE sequence in the E-strand of exon IIIc was deleted. When expressed transiently in COS-7 cells, both constructs with the individual or combined changes gained the ability to bind FGF-7 assessed by both specific binding assays (Figure 8A) and covalent affinity cross-linking (Figure 8B) without effect on the ability to bind FGF-1 and FGF-2. Moreover, a single alteration, K223A, of the C-terminal lysine residue in the invariant D-strand at the exon III junction (Figure 1) in FGFR2βIIIc exhibited a gain in ability to specifically bind FGF-7 (Figure 9A). The poor competition of unlabeled FGF-7 with radiolabeled FGF-1 and the longer exposure time required for detection of the mutants of both FGFR1IIIc and FGFR2IIIc labeled with FGF-7 suggested that the affinity for the gain-of-function constructs for FGF-7 was a fraction of that of wild-type FGFR2IIIb for FGF-7 or FGF-1. However, the binding of FGF-7 was specific and subject to competition with unlabeled FGF-7 and FGF-1 (Figure 8A, data not shown for FGFR2IIIc K223A). These results support the idea that both the fl2 and E domains of the alternately spliced part of exon III, particularly the fl2 domain at the splice junction, play a key role in rejection or acceptance of FGF-7. The results also are consistent with our previous suggestion that the alternately spliced fl2-E domain cooperates with the constitutive fl1-C domain to determine whether it accepts or rejects FGF-7.

Table 1: Effects of Site-Directed Mutations in the FGFR Ectodomain on Binding and Specificity for FGF[a]

construction	domain	effect on FGF binding		
		FGF-1	FGF-2	FGF-7
R1$\beta$$\Delta$E37-E49 (*22*)	acidic box	N	N	N
R1$\alpha$$\Delta$D120-M149 (*16*)	inter I/II	I	I	N
R1$\alpha$$\Delta$E126-E139 (*16*)	acidic box	I	I	N
Ig Module II				
R1βE70A	II-A	N	N	N
R1βK71P (*4*)	II-A	R	R	ND
R1βK71P, K74V (*4*)	II-A	R	R	ND
R1βK71P, K74V, K75E (*4*)	II-A	A	A	ND
R1βK71P, K75E (*4*)	II-A	R	R	ND
R1βE73A	II-A	N	N	N
R1βK74V, K75E (*4*)	II-A	R	R	ND
R1βK83D, K86Q (*4*)	II-bl1-B	R	R	ND
R1βC89S (*22*)	II−B	A	A	ND
R1αC188S (*22*)	II−B	A	A	ND
R1βD135A	II-bl3	R	R	N
R1βY139A	II-bl3	A	A	ND
R1βD157A	II-G	N	N	N
Dimerization Domain				
R1βE160A	inter II/III	N	N	N
R1βS162W	inter II/III	N	N	N
R1βP163R	inter II/III	N	N	N
R1βH164F	inter II/III	R	R	N
Ig Module III				
R1βE185L	III-B	N	R	N
R1βS192I, D193L (*5*)	III-fl1	A	A	ND
R1/R2IIIbS192I, D193L (*5*)	III-fl1	N	N	ND
R1βD193A	III-fl1	N	R	N
R1/R2IIIbD193A	III-fl1	R	A	R
R1βP194L, P196L (*5*)	III-fl1	N	R	N
R1/R2IIIbP194L, P196L (*5*)	III-fl1	N	A	A
R1βH197F (*5*)	III-C	N	N	ND
R1βH203F (*5*)	III-C	N	N	ND
R2βIIIbK223A	III-D	N	ND	N
R2βIIIcK223A	III-D	N	N	G
R1βT224H, A225S	III-fl2	N	N	G
R1/R2IIIbH224T, S225A (*5*)	III-fl2	N	N	A
R1βT224H, A225S, ΔK232E233	III-fl2-E	N	N	G
R1/R2IIIbH224T, S225A, +K232E233 (*5*)	III-fl2-E	N	N	A
R1βD231A	III-E	N	N	N
R1βK232A	III-E	N	N	N
R1$\beta$$\Delta$K232E233	III-E	N	N	G
R1/R2IIIb+K232E233 (*5*)	III-E	N	N	A
R1βC252S (*22*)	III-F	A	A	ND
R1αC341S (*22*)	III-F	A	A	ND

[a] References to published constructs not described in the current study are in parentheses. "Domain" refers to the Ig homology domains described in Figure 1. Numbering is based on the indicated α or β isoform. R1/R2 refers to a chimeric construct of FGFR1β, which contains the exon IIIb sequence from FGFR2 (*5*). N indicates that the alteration had no significant effect on binding (>90% of the binding activity of the wild-type counterpart), A indicates abrogation of specific binding to less than 10% of wild type, R indicates a reduction in degree of binding between 10% and 80% of wild type, I indicates a greater than 2-fold increase in the level of binding (>500% for the mutants indicated), and G indicates a gain in binding from an undetectable base line. ND, not determined.

Specific Residues in the N-Terminus of the Inter-Ig Module II/III Sequence Are Not Required for FGF Binding. The connector sequence between Ig modules II and III and part of the A domain of module III participates in the homeo-interaction between FGFR (*15*). The role of the connector sequence domain in FGF binding remains unclear. Previous results suggest that scrambling both the inter-module and A-strand portions of the connector sequence not only reduced the interaction between FGFR but also abolished FGF binding (*15*). Molecular models of the ternary FGFR complex suggest that the junction of the G strand of Ig module II and the N-terminus of the inter-module sequence may be important for interaction with FGF (Figure 1). To further examine the potential role of individual residues in the G strand from module II and the inter-module connecting sequence domain, we constructed FGFR1 mutants, R1D157L, R1E160L, R1S162W, R1P163R, and R1H165F. When expressed in Sf9 insect cells (Figure 10) or mammalian COS cells (data not shown), R1D157L, R1E160L, R1S162W, and R1P163R bound FGF with an activity indistinguishable from wild-type FGFR1 (Figure 10). In contrast, covalent affinity cross-linking (Figure 10) and Scatchard analysis (not shown) revealed that mutant R1H164F with the alteration toward the C-terminus of the module connector sequence exhibited an apparent K_d of 2000 pM for FGF-1 compared to the 150 pM K_d of wild-type FGFR1β.

DISCUSSION

The ectodomain of the kinase component of the FGFR complex consists of two Ig-like modules II and III split by a connecting sequence (the FGFRβ isoform) which in the presence of heparin or a specific peri-cellular matrix heparan sulfate is sufficient to support the binding of activating FGF polypeptides at maximum affinity (*1*−*3*). Alternate splicing results in a sequence rich in acidic residues ("the acidic box") that is N-terminal to the two modules as well as an additional Ig module I (the FGFRα isoform), the latter of which modifies the affinity for both the binding of heparin and FGF (*16*). A major heparin binding domain has been identified near the N-terminus of module II that is thought to facilitate the binding of FGF to form a ternary complex under physiological conditions (*4*, *11*). In contrast to Ig module II that is invariant, the C-terminal portion of module III is subject to alternate splicing which alters the specificity for FGF. Mutually exclusive splicing of genomic cassettes of exons IIIb and IIIc coding for the C-terminal part of exon III in the FGFR2 gene, which is generally expressed in epithelial cells, is particularly specific in respect to stromal cell-derived FGF-7 and FGF-10 (*1*−*3*, *20*, *24*). Of variants of the four FGFR kinase genes, only the FGFR2IIIb splice variant will bind FGF-7 to any extent. FGF-7 cannot be forced to bind to any of the other isoforms even where they are expressed at high concentrations.

Previously we showed by limited proteolysis and mutation that a duplex of heparin and a fragment of FGFR1 or FGFR2 comprised of Ig module II, the module II/III connector sequence, and 22 amino acid residues of the N-terminus of module III bound FGF-1, FGF-2, and FGF-7 with equal affinity (*5*). Reduction of the portion of Ig module III in the fragment to 9 amino acid residues obliterated binding of all 3 FGFs, suggesting that the sequence domains (bl1-B, see Figure 1) encoded in the 13 deleted residues might be a common requirement for binding of all FGFs. In this report, we show that a duplex of heparin and the isolated Ig module II defined by homology to common C-type Ig motifs also binds FGF-1, FGF-2, and FGF-7 in the absence of flanking sequences. Although the level of binding of FGF-1 to isolated module II is near that of the intact FGFRβ containing two Ig modules, the affinity for FGF-2 and FGF-7 is significantly reduced relative to FGFRβ. This suggests that the connector sequence and the first nine residues, the A-strand, of Ig

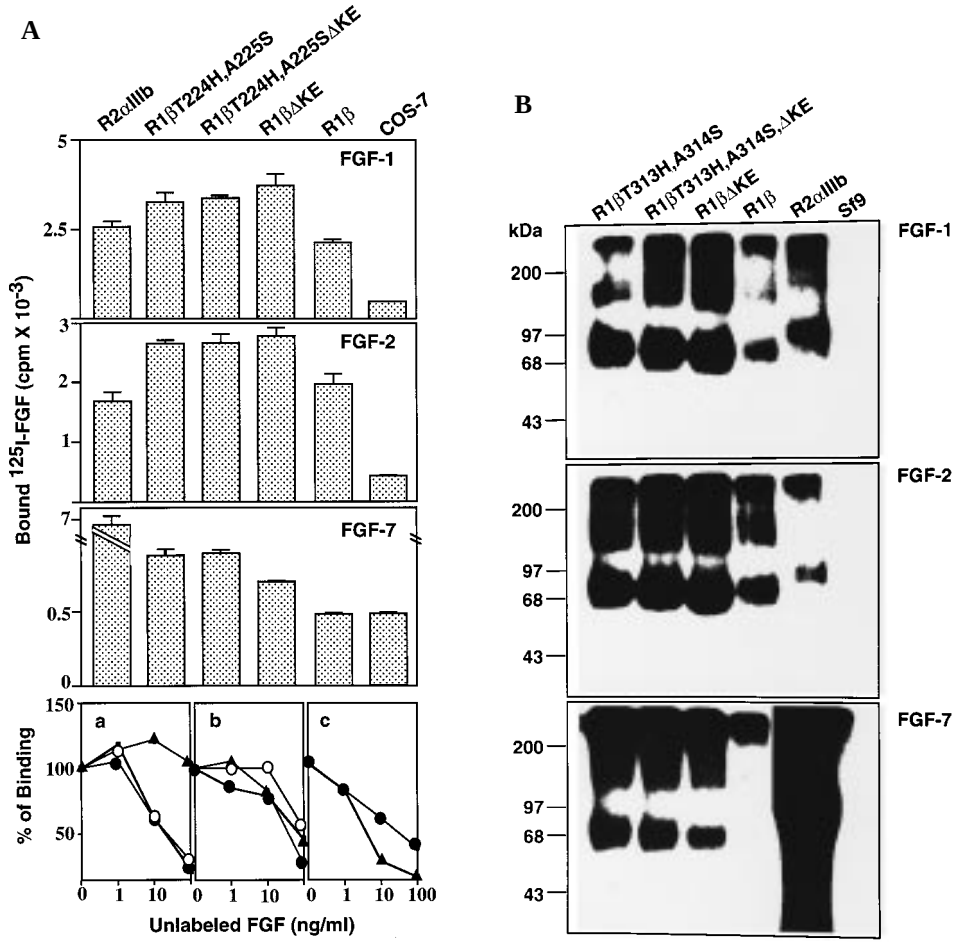

FIGURE 8: Effect of alterations in the alternately spliced fl2-E domain in Ig module III on the binding of FGF-7. The indicated FGFR constructions were expressed transiently in 10^6 COS-7 cells as described in Figure 6. Five hours after transient transfection, the cells were distributed into three 6 cm culture dishes and cultured for 2 days before use in binding assays containing radiolabeled FGF-1, FGF-2, or FGF-7 as indicated. Specifically bound FGF was determined by total detergent-extractable count (A) and SDS−PAGE and autoradiography (B) after incubation with DSS. The data in (A) were means of duplicates with variations indicated. The bottom panel in (A) with frames a−c illustrates the specificity of the binding shown in the upper panels. Competition of the indicated amount of unlabeled FGF-1 (solid circles), FGF-2 (open circles), or FGF-7 (triangles) with the binding of radiolabeled FGF-1 (a and b) or FGF-7 (c) to FGFR2βIIIb (b) and FGFR1βT224H,A225S (a and c) expressed in COS-7 cells was determined in assays of a total volume of 250 μL containing 2 ng/mL radiolabeled FGF. The data are the mean of duplicates. 100% values for the lower panel were 18 and 1.5 fmol for FGF-1 and FGF-7, respectively. In (B), the FGF-1 and FGF-2 panels were from films exposed for 24 h while the panel from FGF-7 is from film exposed for 10 days. The main band of the overexposed wild-type FGFR2αIIIb-FGF-7 complex is at 83 kDa (65 kDa plus FGF-7).

module III interfere with the binding of all three FGFs to module II. However, together with the 13 additional residues spanning most of the bl1-B domain of module III, the sequence plays a role, possibly as a secondary binding domain, which contributes to the affinity of specifically FGF-2 and FGF-7 to the heparin−module II base. The complex of heparin and isolated module II appears sufficient for maximum binding of FGF-1. Although other mutants are under study, one mutation, E185A, in the B-strand of module III in FGFR1β that was predicted by modeling to obliterate a favorable charge interaction with specifically FGF-2 yielded the expected experimental result, a decrease in affinity of the fragment for FGF-2 without effect on FGF-1 or FGF-7 (Table 1). We conclude that a complex of heparan sulfate and Ig module II is necessary and sufficient for binding of FGF-1 and necessary, but cooperative with additional FGFR domains to achieve maximal affinity for FGF-2 and FGF-7. These results differ quantitatively from those of Cheon et al. (*25*), who showed in binding assays using soluble FGFR2 constructions that isolated module II fused at the C-terminus with the two constant Ig units of the immunoglobulin heavy chain was sufficient for binding of FGF-1, but failed to demonstrate the binding of FGF-7. Instead FGF-7 bound significantly, but at lower affinity than for FGFR2βIIIb, to a construction containing the connector sequence between modules II and III and module III fused to the two Ig units of the constant heavy chain of immunoglobulins. It was concluded that modules II and III are specific for FGF-1 and FGF-7, respectively. However, the fact that each is mutually competitive for binding to FGFR2βIIIb suggests that the two FGFs share binding sites overall. The failure to demonstrate the binding of FGF-7 to isolated module II might be due to insensitivity of binding assays that do not employ direct covalent affinity labeling, the more stringent requirement of heparin for binding to isolated module II, or interference with FGF-7 binding of the sequences C-terminal to module II in the particular constructions. In this report, we show that FGF-7 fails to bind detectably to isolated Ig module IIIb under our most sensitive assay conditions. However, the results of experiments that will be reported in detail elsewhere suggest that the Ig II/III connector sequence and the A-strand sequence of module III, which is required

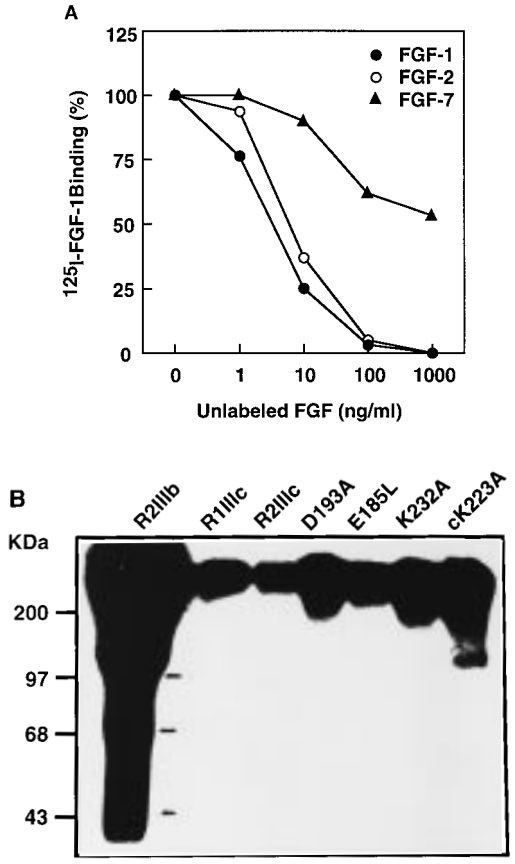

FIGURE 9: Gain of FGF-7 binding by mutation in the D-fl2 domain at the exon III junction. (A) A mutant of FGFR2IIIc (cK223A) with substitution of Lys-223 with alanine was expressed in baculoviral-infected Sf9 cells, and the competition of unlabeled FGF-1, FGF-2, and FGF-7 with radiolabeled FGF-1 was compared. (B) Radiolabeled FGF-7 (5 ng/mL) in assays of 100 μL containing 5×10^4 cells expressing the indicated recombinant products (Figure 1, Table 1) was bound and covalently cross-linked with DSS and followed by analysis by SDS−PAGE and autoradiography. Autoradiographs were exposed for 2.5 days. The FGFR2IIIb and FGFR2IIIcK223A expression product has a mass of 92 kDa and when bearing radiolabeled FGF-7 is the band at 107 kDa in the overexposed lane at the left and the single band in the lane at the right. A significant additional FGF-7-labeled band in the overexposed wild-type lane is at 73 kDa, which is the truncated ectodomain resulting from proteolysis as described (9).

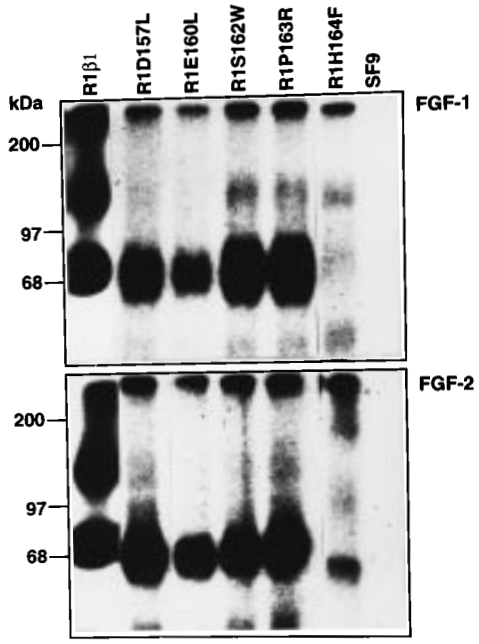

FIGURE 10: Lack of effect of point mutations in the connecting sequence between modules II and III on FGF-1 and FGF-2 binding. The indicated FGFR constructions were expressed in 10^6 Sf9 cells and immobilized on protein A−Sepharose beads through anti-FGFR antiserum A40 (9). The amount of antigen was assessed in 90% of the sample prior to binding analysis with anti-FGFR1 monoclonal M17A3. Ten percent of the beads were used in binding assays containing ^{125}I-FGF-1 or FGF-2 followed by covalent cross-linking with DSS, determination of the total count by a γ-counter, and then analysis by SDS−PAGE and autoradiography. Full-length FGFR1β1 labeled with one FGF (left lane) has a mean apparent mass of 108 kDa. The lower band at 70 kDa is a truncate of the ectodomain resulting from proteolysis (9). Products of all five of the other membrane-anchored constructs which have a short intracellular domain have a mass of 50 kDa resulting in a radiolabeled band of about 68 kDa.

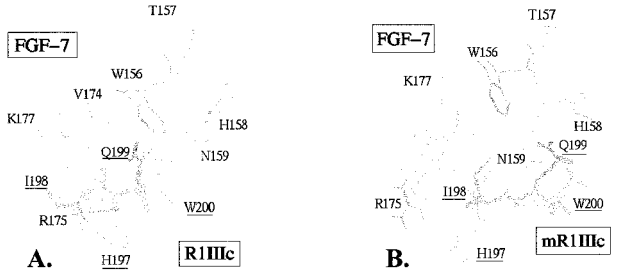

FIGURE 11: Relief of conflict between FGF-7 and the fl1-C domain of FGFR1IIIc by mutation of specific sites in the fl2 and E domains to those in exon IIIb. (A) An experimentally impossible model of FGF-7, heparin, and FGFR1βIIIc (R1IIIc) constructed as described under Materials and Methods indicates a conflict between adjacent, but discontinuous domains in FGF-7 (thin lines) and the fl1-C domain of FGFR1βIIIc (thick lines). (B) Substitution of the FGFR1βIIIc fl2 TA dipeptide sequence with the HS sequence in the IIIb exon of FGFR2 and FGFR1 and deletion of the KE sequence in the E-strand (mR1IIIc) remove the conflicting interaction. Numbered residues in FGFR are underlined.

for interaction between FGFR ectodomains (*15*), enhances the affinity of FGF-2 and FGF-7 to module II. If this domain or the dimerization of it directly contributes to the primary site, or provides a partial binding site, then combined with module IIIc or IIIb the inter-module sequence may have sufficient affinity to bind FGF-2 and FGF-7, respectively, in the absence of module II. Our preliminary results suggest that possibility.

A complex of heparin and Ig module II plus the connector sequence and 22 residues of the N-terminus of module III supports the binding of FGF-1, FGF-2, and FGF-7 equal to intact FGFRβ (5). However, the extension beyond that point by just a few amino acid residues which comprise the constitutive fl1-C domain abolishes the binding of FGF-7 without effect on FGF-1 and FGF-2 (5). We concluded that the fl1-C sequence domain plays a major role in the restriction of FGF-7 binding relative to FGF-1 and FGF-2 but, since it is constitutive, its orientation must be modified by downstream sequences in the IIIb exon to permit binding of FGF-7. A more detailed and refined atomic model of a ternary complex of FGF-7, heparin, and FGFR1βIIIc which indicates a severe conflict between FGF-7 and FGFR1βIIIc at the fl1-C domain, particularly with residues Pro-196 to Gln-199, supports this idea (Figure 11A). A previous report showed that the substitution of the exon IIIb H224S225 residues of FGFR2IIIb with exon IIIc residues T224A225

from FGFR1IIIc or insertion of IIIc residues K232E233 into the IIIb exon specifically abolished the binding of FGF-7 without disruption of the binding of FGF-1 and FGF-2 (*5*). These results suggested that residues in both the fl2 and E domain of the alternately spliced section of Ig module III play a role in abrogating the rejection of FGF-7 and make the sites strong candidates for the indirect modification of the restrictive effects of the fl1-C domain. Residues T226A227 in the IIIc exon of FGFR1 were replaced with the HS of IIIb, and the exon IIIc dipeptide KE was deleted in exon IIIc in the model of a ternary complex of FGFR1βIIIc, heparin, and FGF-7 (Figure 11B). After performance of molecular dynamics and energy minimization, the conflict of FGF-7 with the fl1-C domain was notably relieved without a significant change in the global relationship between Ig modules. Experimental test of the prediction revealed that either substitution of TA with the HS of FGFR2IIIb or deletion of KE from FGFR1IIIc confers the ability to detectably bind FGF-7 on FGFR1βIIIc, an isoform that otherwise absolutely rejects FGF-7 under all conditions. Although both alterations in the fl2-E domain of exon IIIc independently conferred a significant increase in the binding of FGF-7 to FGFR1IIIc, the TA to HS substitution at the splice junction of the alternate exons at the D strand−fl2 boundary appeared quantitatively more effective. The failure of point mutation of the single lysine residue of the KE sequence (K232A) in exon IIIc (Figure 9A, Table 1) to confer FGF-7 binding suggested that deletion of the two residues underpins the change rather than the unfavorable charge interaction between the side chain of Lys-232 and basic residues specifically in FGF-7 that was suggested by our model. That the D-fl2 junction is the more important contributor was further supported by the gain in FGF-7 binding conferred by mutation to alanine of the constitutive Lys-311 at the C-terminus of the D strand of module IIIc. Since the alternately spliced fl2-E domain is dispensable for FGF-7 binding in absence of the fl1-C domain of Ig module III, we conclude from these combined results that the fl2-E domain of the IIIb exon plays an indirect role in abrogating restrictions on FGF-7 binding imposed by the constitutive fl1-C domain.

The hypothetical models shown in Figure 11 suggest that the primary conflict of FGF-7 with the fl1-C domain of FGFRIIIc lies in the unique sequence between β-strands 10 and 12. We refer to this characteristic region as the "glycine box" (G-box) which has been shown to be α-helical in FGF-2 in solution in contrast to the β-strand conformation in crystals (*26*). Our model also predicts additional, but less severe, conflicts between the inter-β-strand 9 and 10 sequence in FGF-7 with the fl1-C domain of FGFR1IIIc. In a separate report, we show that replacement of the C-terminal domain of FGF-7 with that of FGF-1 and specific alterations in the G-box confer ability on FGF-7 to bind with a significant affinity to FGFR1IIIc (*21*).

In summary, these results are consistent with a conformational model of the FGFR complex in which Ig module II anchored to peri-cellular matrix heparan sulfate chains of proteoglycans through divalent cations is the base, common, and indispensable primary binding site for all FGFs. This is further supported by the fact that none of over 30 autosomal dominant, gain-of-function mutations in FGFR that cause developmental cranio-facial and skeletal abnormalities occur within module II (*27*). Such mutations are likely to be null or haploid insufficiency mutations due to the stringent requirement for an intact module II structure for both heparan sulfate and FGF binding. The experiments reported here were performed using Ig module II from FGFR1. Preliminary results with module II from FGFR2 suggest that qualitatively the isolated module when complexed with heparin binds FGF-1, FGF-2, and FGF-7. Whether isolated modules II of the four different FGFRs exhibit a difference in affinity for different FGFs independent of or cooperative with heparan sulfate in the heparan sulfate−FGFR duplex is under investigation. From the current results, we propose that secondary interactions of FGFs other than FGF-1 docked onto the module II−heparan sulfate duplex may interact with secondary domains in the connector sequence between modules II and III of FGFR and the N-terminus of module III to alter the affinity for particular FGFs other than FGF-1. Since this sequence domain includes a dimerization interface, the effect on affinity might be due to the composite structure formed by interaction between two FGFRs rather than the individual sequence domain within a monomer. This is in addition to interactions of sequence domains in module III further downstream as described in this and previous reports (*5*)

We have suggested previously that the relationship of a mobile module III and the fixed heparan sulfate−module II complex determines the proximity of the intracellular kinases, which are enzyme−substrate activators of each other through trans-phosphorylation (*3, 11, 15*). FGF or gain-of-function mutations downstream of Ig module II lock a mobile module III into a conformation where the kinases are in sustained proximity. The gain-of-function mutations in the connector sequence and module III on kinase activity are independent of FGF binding, but fortuitously affect FGF binding dependent on whether the mutation causes module III to interfere with the binding of FGF to the complex of heparan sulfate and module II. As demonstrated in this report and elsewhere (*21, 28*), the fact that some gain-of-function mutants retain and some lose FGF binding activity supports this idea.

To date, the generation of direct structural information about the ectodomain of the FGFR complex has been hampered by insolubility, low yield, and low activity of the two-module structure of FGFRβ from bacterial expression systems. This may be due to requirement for a precise conformational relationship between modules II and III and the requirement for heparan sulfate in folding or maturation which is absent in lower organisms. The finding that a complex of isolated Ig module II and heparin exhibits full activity for the binding of FGF-1 and significant ability to bind FGF-2 and FGF-7 may simplify direct determination of the nature of the FGFR complex as well as identification of the native heparan sulfate subunit by its use in affinity chromatography.

REFERENCES

1. Jaye, M., Schlessinger, J., and Dionne, C. A. (1992) *Biochim. Biophys. Acta 1135*, 185−199.
2. Johnson, D. E., and Williams, L. T. (1993) *Adv. Cancer Res. 60*, 1−41.
3. McKeehan, W. L., Wang, F., and Kan, M. (1998) *Prog. Nucleic Acid Res. Mol. Biol. 59*, 135−176.

4. Kan, M., Wang, F., Xu, J., Shi, E., Crabb, J. W., Hou, J., and McKeehan, W. L. (1993) *Science 259*, 1918−1921.
5. Wang, F., Kan, M., Xu, J., Yan, G., and McKeehan, W. L. (1995) *J. Biol. Chem. 270*, 10222−10230.
6. Ornitz, D. M., Xu, J., Colvin, J. S., McEwen, D. G., MacArthur, C. A., Coulier, F., Gao, G., and Goldfarb, M. (1996) *J. Biol. Chem. 271*, 15292−15297.
7. Pantoliano, M. W., Horlick, R. A., Springer, B. A., Van Dyk, D. E., Tobery, T., Wetmore, D. R., Lear, J. D., Nahapetian, A. T., Bradley, J. D., and Sisk, W. P. (1994) *Biochemistry 33*, 10229−10248.
8. Springer, B. A., Pantoliano, M. W., Barbera, F. A., Gunyuzlu, P. L., Thompson, L. D., Herblin, W. F., Rosenfeld, S. A., and Book, G. W. (1994) *J. Biol. Chem. 28*, 26879−26884.
9. Xu, J., Nakahara, M., Crabb, J. W., Shi, E., Matuo, Y., Fraser, M., Kan, M., Hou, J., and McKeehan, W. L. (1992) *J. Biol. Chem. 267*, 17792−17803.
10. Schlessinger, J., Lax, I., and Lemmon, M. (1995) *Cell 83*, 357−360.
11. Kan, M., Wang, F., Kan, M., To, B., Gabriel, J. L., and McKeehan, W. L. (1996) *J. Biol. Chem. 271*, 26143−26148.
12. Luo, Y., Gabriel, J. L., Wang, F., Zhan, X., Maciag, T., Kan, M., and McKeehan, W. L. (1996) *J. Biol. Chem. 271*, 26876−26883.
13. Herr, A. B., Ornitz, D. M., Sasisekharan, R., Venkataraman, G., and Waksman, G. (1997) *J. Biol. Chem. 272*, 16382−16389.
14. Moy, F. J., Safran, M., Seddon, A. P., Kitchen, D., Bohlen, P., Aviezer, D., Yayon, A., and Powers, R. (1997) *Biochemistry 36*, 4782−4791.
15. Wang, F., Kan, M., McKeehan, K., Jang, J.-H., Feng, S., and McKeehan, W. L. (1997) *J. Biol. Chem. 272*, 23887−23895.
16. Wang, F., Kan, M., Yan, G., Xu, J., and McKeehan, W. L. (1995) *J. Biol. Chem. 270*, 10231−10235.
17. Hou, J., Kan, M., McKeehan, K., McBride, G., Adams, A., and McKeehan, W. L. (1991) *Science 251*, 665−668.
18. Wang, F., Kan, M., and McKeehan, W. L. (1995) *BioTechniques 19*, 556−559.
19. Shi, E., Kan, M., Xu, J., Hou, J., McBride, G., and McKeehan, W. L. (1993) *Mol. Cell. Biol. 1*, 3907−3918.
20. Feng, S., Wang, F., Matsubara, A., Kan, M., and McKeehan, W. L. (1997) *Cancer Res. 57*, 5369−5378.
21. Luo, Y, Lu, W., Mohamedali, A., Jang, J., Jones, R. B., Gabriel, J. L., Kan, M., and McKeehan, W. L. (1998) *Biochemistry 37*, 16506−16515.
22. Hou, J., Kan, M., Wang, F., Xu, J.-M., Nakahara, M., McBride, G., McKeehan, K., and McKeehan, W. L. (1992) *J. Biol. Chem. 267*, 17804−17808.
23. Fong, S., Hamill, S. J., Proctor, M., Freund, S. M. V., Benian, G. M., Chothia, C., Bycroft, M., and Clarke J. (1996) *J. Mol. Biol. 264*, 624−639.
24. Igarashi, M., Finch, P. W., and Aaronson, S. A. (1998) *J. Biol. Chem. 273*, 13230−13235.
25. Cheon, H.-G., LaRochelle, W. J., Bottaro, D. P., Burgess, W. H., and Aaronson, S. A. (1994*) Proc. Natl. Acad. Sci. U.S.A. 91*, 989−993.
26. Moy, F. J., Seddon, A. P., Böhlen, P., and Powers, R. (1996) *Biochemistry 35*, 13552−13561.
27. Muenke, M., and Schell, U. (1995) *Trends Genet. 11*, 308−313.
28. Neilson, K. M., and Friesel, R. E. (1995) *J. Biol. Chem. 270*, 26037−26040.

BI981758M